JACS
JOURNAL OF THE AMERICAN CHEMICAL SOCIETY
Article
Cite This: J. Am. Chem. Soc. 2017, 139, 15168-15175
pubs.acs.org/JACS

In Search of the Perfect Photocage: Structure–Reactivity Relationships in *meso*-Methyl BODIPY Photoremovable Protecting Groups

Tomáš Slanina,[†,‡] Pradeep Shrestha,[§,⊥] Eduardo Palao,[†,⊥] Dnyaneshwar Kand,[∥] Julie A. Peterson,[§] Andrew S. Dutton,[§] Naama Rubinstein,[∥] Roy Weinstain,*[,∥] Arthur H. Winter,*[,§] and Petr Klán*[,†]

[†]Department of Chemistry and RECETOX, Faculty of Science, Masaryk University, Kamenice 5, 625 00, Brno, Czech Republic
[‡]Institute of Organic Chemistry and Chemical Biology, Goethe University Frankfurt, 60323 Frankfurt am Main, Germany
[§]Department of Chemistry, Iowa State University, 1608 Gilman Hall, Ames, Iowa 50010, United States
[∥]School of Plant Sciences and Food Security, Faculty of Life Sciences, Tel-Aviv University, Tel-Aviv 6997801, Israel

Supporting Information

ABSTRACT: A detailed investigation of the photophysical parameters and photochemical reactivity of *meso*-methyl BODIPY photoremovable protecting groups was accomplished through systematic variation of the leaving group (LG) and core substituents as well as substitutions at boron. Efficiencies of the LG release were evaluated using both steady-state and transient absorption spectroscopies as well as computational analyses to identify the optimal structural features. We find that the quantum yields for photorelease with this photocage are highly sensitive to substituent effects. In particular, we find that the quantum yields of photorelease are improved with derivatives with higher intersystem crossing quantum yields, which can be promoted by core heavy atoms. Moreover, release quantum yields are dramatically improved by boron alkylation, whereas alkylation in the *meso*-methyl position has no effect. Better LGs are released considerably more efficiently than poorer LGs. We find that these substituent effects are additive, for example, a 2,6-diiodo-*B*-dimethyl BODIPY photocage features quantum yields of 28% for the mediocre LG acetate and a 95% quantum yield of release for chloride. The high chemical and quantum yields combined with the outstanding absorption properties of BODIPY dyes lead to photocages with uncaging cross sections over 10 000 M^{-1} cm^{-1}, values that surpass cross sections of related photocages absorbing visible light. These new photocages, which absorb strongly near the second harmonic of an Nd:YAG laser (532 nm), hold promise for manipulating and interrogating biological and material systems with the high spatiotemporal control provided by pulsed laser irradiation, while avoiding the phototoxicity problems encountered with many UV-absorbing photocages. More generally, the insights gained from this structure–reactivity relationship may aid in the development of new highly efficient photoreactions.

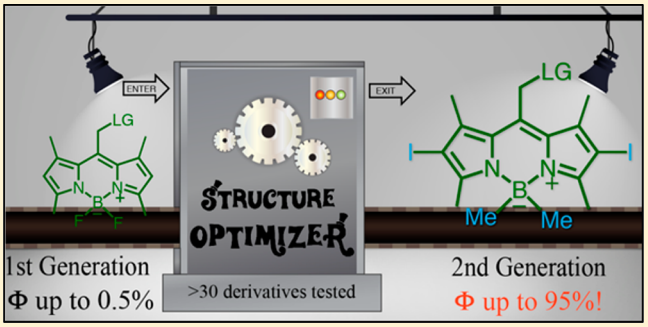

INTRODUCTION

Photoremovable protecting groups (PPGs) are a useful tool for temporary protection of a functional group from undesired chemical transformations.[1] A substantial research effort has been devoted to the development and applications of UV-light-absorbing PPGs, such as 2-nitrobenzyl (*o*NB),[2] benzoinyl (desyl),[3] 4-hydroxyphenacyl,[4,5] and coumarinyl[6] moieties. The concept of PPGs is especially useful in biological research, where PPGs, often referred to as "caged compounds", allow for release of desired biologically active compounds (e.g., ATP,[7] GABA[8]) with high spatial and temporal resolution.[9] However, UV light has low tissue penetration and can cause unwanted photochemical transformations, such as thymine dimerization and subsequent DNA damage.[10] PPGs absorbing biologically/chemically benign visible light are thus highly desired for biological and medical applications.

Visible-light-absorbing PPGs have been reported only recently because the excitation energy delivered by visible light is generally too low for bond cleavage.[1,11] The first attempts to design a visible-light-absorbing PPGs were based on organometallic ruthenium complexes used for caging of GABA with the absorption maximum at 447 nm.[12,13] Some of us have recently introduced the first fully organic visible-light-absorbing PPGs based on the xanthene (suitable for protection of halides, carboxylates, and phosphates)[14] and pyronin[15] chromophores. Another strategy has been used for coumarin-based PPGs. A derivative of 7-diethylaminocoumarin-4-ylmethyl PPG was prepared by Ellis-Davies and co-workers in 2013.[16] It has a strong absorption at 450 nm (ε_{450} = 43 000

Received: August 11, 2017
Published: October 17, 2017

DOI: 10.1021/jacs.7b08532
J. Am. Chem. Soc. 2017, 139, 15168–15175

M^{-1} cm^{-1}) and efficiently (Φ = 0.78) uncages *c*AMP. Substitution of the carbonyl oxygen of a lactone functionality with sulfur leads to 7-diethylamino-4-thiocoumarinylmethyl PPG,[17] which has an even more red-shifted absorption (λ_{max} = 470 nm) and higher molar absorption coefficient (ε_{500} > 10 000 M^{-1} cm^{-1}) even at 500 nm, with a quantum yield of leaving group (LG) release $\Phi \approx 5 \times 10^{-3}$. In 2014, Urano and co-workers designed a 4-aryloxy-BODIPY-based PPG absorbing at 500 nm for protection of various electron-rich phenols.[18] The mechanism of the deprotection includes photoinduced electron transfer from the electron rich aryl group to the BODIPY moiety which undergoes self-immolative cleavage. Recently, Urano and co-workers used the photolability of 2,6-sulfonamide-substituted BODIPYs for GABA caging.[19] The mechanism of the deprotection is based on intramolecular electron transfer and subsequent fission of sulfonamide moiety. The group of Schnermann has introduced a cyanine-based PPG[20] capable of cleavage in the near-IR region (690 nm) which lays in the tissue-transparent window.[21] The compound has been used as a photolabile linker for antibody-drug conjugates. The mechanism of the photodeprotection is based on [2+2] photooxidation[22] and subsequent hydrolytic cleavage of the LG. Recently, some of us introduced transition-metal-free carbon monoxide-releasing molecules (CORMs) based on xanthene[23] as well as BODIPY chromophores, which are activatable by visible-to-NIR (up to 730 nm) light.[24] The groups of Winter[25] and Weinstain[26] have concurrently introduced the novel *meso*-methyl BODIPY PPGs. It was suggested that the LG release occurs via a photochemical S_N1 reaction via a carbocation intermediate and the subsequent nucleophilic attack of the solvent (Scheme 1).

Scheme 1. Photorelease of a Leaving Group (LG) from the BODIPY Cage

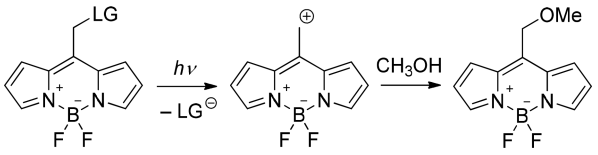

The *meso*-methyl BODIPY derivatives feature many ideal characteristics of a photocage; BODIPYs are biologically benign, are excellent chromophores (ε > 50 000 M^{-1} cm^{-1}), are thermally stable in the dark, are synthetically accessible, have no chiral centers, and have tunable absorptions throughout the visible/near-IR region. However, a drawback is that the currently known *meso*-methyl BODIPY photocages have low quantum yields of photorelease (Φ_r). We hypothesized that a systematic structure–activity relationship (SAR) study of *meso*-methyl BODIPY photocages would provide structural and mechanistic insights that could be translated into rational design of improved versions.

In this work, we report a systematic SAR study on 32 *meso*-methyl BODIPY photocages and assessment of their photophysical and photochemical properties. Efficiencies of the LG release were evaluated using both steady-state and transient absorption spectroscopies as well as computational analyses to find the optimal structural features. We identified two structural motifs, each leading to a significant improvement in quantum yields of photorelease. Based on these findings, we rationally incorporated the two identified structural motifs in a single BODIPY photocage, resulting in an optimized version featuring superb quantum yields and strong absorption properties. These characteristics make the optimized BODIPY photocages an exceptionally compelling alternative to the commonly used UV- or visible-light-absorbing photocages.

RESULTS AND DISCUSSION

2,6-Dihalogen Substitution. Introduction of heavy atoms into PPG structures is an obvious effective strategy to improve the latter photoreaction efficiency through increase of the molecules' intersystem crossing (ISC) efficiency if the LG is liberated from the triplet excited state. To explore whether this strategy would prove effective in the case of *meso*-methyl BODIPY photocages, we synthesized three sets of 2,6-dihalogen BODIPY derivatives (**1**–**3**, **a**–**c**, Figure 1), each

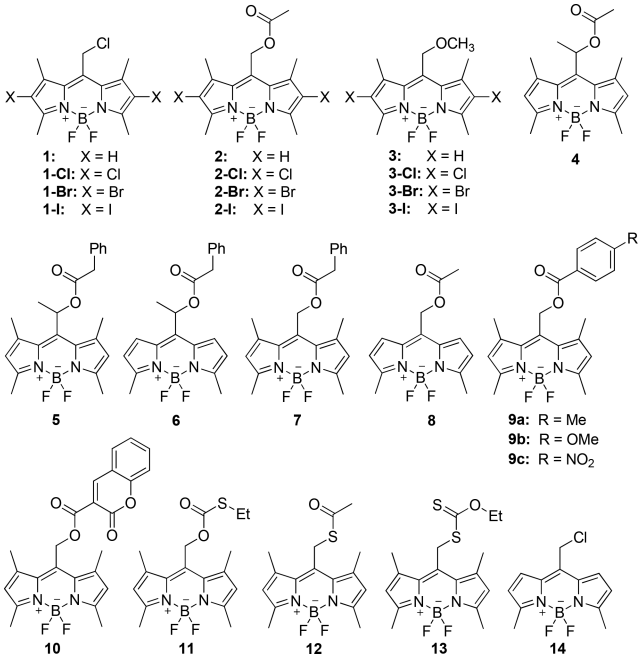

Figure 1. Structures of BODIPY photocages synthesized and evaluated in this study.

bearing a different model LG on its *meso* position, by directly reacting the corresponding 2,6-dihydrogen BODIPY with *N*-chloro-, *N*-bromo-, or *N*-iodo-succinimide (Supporting Information). The spectroscopic properties of these 12 BODIPYs are summarized in Table 1.

The absorption maxima (λ_{max}^{abs}) of the 2,6-dihalogen derivatives are bathochromically shifted (544–556 nm) compared to their non-halogen analogues (529–534 nm), and they maintain high molar absorption coefficients (ε), in the range of (3–7) × 10^4 M^{-1} cm^{-1} (Table 1). The fluorescence quantum yields (Φ_f) of the 2,6-dihalogened BODIPYs decrease in an inverse proportion to the atomic number of the 2,6-substituents (H < Cl < Br < I), presumably, due to increased intersystem crossing (ISC) efficiency caused by the presence of the heavy atoms.[28] To verify that the ISC indeed increases in these specific molecules, their quantum yields of ISC (Φ_{ISC}) were directly measured in degassed methanol using transient absorption spectroscopy (Table 1 and Supporting Information).[29,30] ISC was found to be relatively inefficient in 2,6-dihydrogen derivatives **1** and **2**; its values were below the detection limit of our pump–probe setup (Φ_{ISC} < 0.05). In contrast, the corresponding 2,6-dihalogen analogues exhibited

DOI: 10.1021/jacs.7b08532
J. Am. Chem. Soc. 2017, 139, 15168–15175

Table 1. Photophysical Properties and Photoreaction Quantum Yields for 2,6-Dihalogen BODIPYs[a] and Their Non-halogenated Analogues[a]

	absorption		emission			ISC[b]	photoreaction[c]	
compd	λ_{max}^{abs}/nm	ε/M^{-1} cm^{-1}	λ_{max}^{f}/nm	Φ_f/%	τ_f/ns	Φ_{ISC}/%	Φ_r^{aer}/%	Φ_r^{deg}/%
1	523	44 400	534	19.5 ± 1.5	3.57 ± 0.06	<0.05	1.62 ± 0.11	2.37 ± 0.18
1-Cl	549	34 600	566	16.7 ± 1.0	n.d.	12 ± 1	9.48 ± 0.7	20.34 ± 2.1
1-Br	549	55 700	564	10.5 ± 0.5	n.d.	n.d.	27.1 ± 3.3	50.6 ± 5.7
1-I	556	59 300	574	1.2 ± 0.1	n.d.	n.d.	44.5 ± 5.0	80.5 ± 8.1
2	517	71 000	529	73.4 ± 0.8	6.47 ± 0.11	<0.05	0.14 ± 0.01	0.34 ± 0.02
2-Cl	544	48 000	562	67.5 ± 1.8	6.26 ± 0.10	22 ± 3	0.29 ± 0.02	0.74 ± 0.06
2-Br	545	56 300	565	15.5 ± 0.9	1.67 ± 0.05	54 ± 4	0.70 ± 0.07	1.47 ± 0.12
2-I	553	49 000	575	1.8 ± 0.1	0.31 ± 0.02	84 ± 3	0.99 ± 0.10	2.35 ± 0.22
3	515	63 000	533	92.7 ± 0.6	6.66 ± 0.12	<0.05	0.02 ± 0.001	0.04 ± 0.001
3-Cl	541	37 800	565	87.1 ± 1.5	6.30 ± 0.13	24 ± 3	0.04 ± 0.004	0.09 ± 0.008
3-Br	542	57 400	564	16.2 ± 0.5	1.93 ± 0.08	55 ± 4	0.10 ± 0.009	0.32 ± 0.02
3-I	549	49 500	573	1.7 ± 0.1	0.30 ± 0.01	85 ± 3	0.25 ± 0.02	0.63 ± 0.04

[a]Solutions in methanol, $c \approx (1-10) \times 10^{-6}$ M. n.d. = not determined. [b]Determined from six independent measurements; degassed solutions; excitation wavelength = 532 nm; E_{pulse} = 240 mJ. [c]Determined by irradiation at 365 nm (compounds **1**, **2**, **1-Cl**, and **2-Cl**) and 507 nm (all other compounds), using ferrioxalate[27] (λ_{irr} = 365 nm) and xanthene-9-carboxylic acid[23] (λ_{irr} = 507 nm) as actinometers. aer = aerated and deg = degassed solutions.

Table 2. Photophysical Properties and Photoreaction Quantum Yields for Secondary *meso*-Methyl BODIPY Photocages and Their Primary Analogues[a]

	absorption		emission			photoreaction[b]	
compd	λ_{max}^{abs}/nm	ε^{c}/M^{-1} cm^{-1}	λ_{max}^{f}/nm	Φ_f/%[d]	τ_f/ns[c]	Φ_r^{aer}/%[d]	Φ_r^{deg}/%[d]
2[e]	517	71 000	529	73.4 ± 0.8	6.47 ± 0.11	0.14 ± 0.01	0.34 ± 0.02
4	511	60 800	528	2.5 ± 0.1	n.d.	0.12 ± 0.01	0.28 ± 0.02
5	513	74 300	530	2.6 ± 0.1	2.81 ± 0.07	0.13 ± 0.01	0.29 ± 0.02
6	518	66 800	529	69.5 ± 0.6	6.05 ± 0.15	0.15 ± 0.01	0.30 ± 0.02
7	514	104 400	526	95.8 ± 0.3	n.d.	0.15 ± 0.01	0.32 ± 0.02
8	519	57 900	530	86.2 ± 0.2	n.d.	0.11 ± 0.01	0.22 ± 0.01

[a]Solutions in methanol, $c \approx (1-10) \times 10^{-6}$ M. n.d. = not determined. [b]Determined by irradiation at 507 nm using xanthene-9-carboxylic acid[23] (λ_{irr} = 507 nm) as actinometer. aer = aerated and deg = degassed solutions. [c]Determined from three independent measurements. [d]Determined from at least five independent measurements; [e]Data for **2** are repeated from Table 1.

an efficient ISC; Φ_{ISC} increased (as Φ_f simultaneously decreased) in the order of H < Cl < Br < I substitution (e.g., <0.05, 22, 54, and 84% for **2**, **2-Cl**, **2-Br**, and **2-I**, respectively). The representative transient spectra of the triplet state (Figures S1–S4) resembled those previously determined for 2,6-halogen- and 2,6-chalcogen-containing BODIPYs.[31] Notably, **1-Br** and **1-I** were highly photoreactive, preventing determination of their Φ_{ISC}. The Φ_{ISC} value of 0.8 was found for **2-I**, which is consistent with data obtained for the analogous 2,6-diiodo BODIPYs.[32] The nonradiative decay values $\Phi_{nr} = 1 - (\Phi_{ISC} + \Phi_f)$ for the excited singlet states in the series of the derivatives **2** thus range between 0.1 and 0.3. These data confirm that ISC in *meso*-methyl BODIPYs is increased by introduction of 2,6-dihalogen substituents.

We found that the LGs are released quantitatively from several representative derivatives upon exhaustive irradiation in aerated methanolic solutions (**2**, **5**–**10**, **16**, and **18a**; Table S2 and ref 25). It rules out side reactions that would convert the BODIPY chromophore into a nonreleasable derivative.

The photoreaction efficiency was determined for all 12 derivatives in both aerated and degassed solutions (Φ_r^{aer} and Φ_r^{deg}, respectively) using ferrioxalate[27] (λ_{irr} = 365 nm) and xanthene-9-carboxylic acid[23] (λ_{irr} = 507 nm) as actinometers (Tables 1 and 2). Following irradiation in methanol ($c \approx 1 \times 10^{-5}$ M, except **3** (*vide infra*)) using 365, 490, and 507 nm monochromatic light, the release of the LGs was monitored using HPLC and/or ^{1}H NMR (see Supporting Information). It can be clearly observed that both Φ_r^{aer} and Φ_r^{deg} increased proportionally to Φ_{ISC} for all three BODIPY sets (Table 2 and Figure S5). Remarkably, 2,6-diiodo derivatives demonstrated dramatic ~10–20-fold increase in their photoreaction efficiency compared to the previously reported, non-halogenated BODIPY photocages.[25,26] In addition, the quantum yields of the LG release was measured for selected derivatives (Table S3) to show that LG liberation efficiency corresponds to formation of the methoxy derivative **3**.

All degassed samples gave a higher Φ_r^{deg} compared to those in aerated solutions (Φ_r^{aer}) by a factor of ~2. Thus, if singlet oxygen is simultaneously produced by BODIPY triplet-state sensitization, it did not affect the photoproduct formation (that is, no alternative decomposition of the starting material was observed). This means that oxygen present in the samples only quenched the productive excited state; the BODIPY cages do not undergo any side reactions in aerated solutions and thus could be effectively used in biological environment.

Monitoring the photoreaction progress has also enabled us to identify its photoproducts. The methoxy derivative **3** and its halogen analogues were found as the major photoproducts in irradiated methanolic solutions (in accord with earlier findings by Winter[25] and Weinstain[26]), in some cases formed quantitatively (Figure S6). It is worth noting that the absorption spectrum of the photoproducts partially overlaps

DOI: 10.1021/jacs.7b08532
J. Am. Chem. Soc. 2017, 139, 15168–15175

with those of the starting BODIPYs. Thus, they can act as an optical filter. However, compound **3** is not photostable but undergoes a relatively inefficient photochemical destruction of the BODIPY core (Φ_R^{deg} = 0.04%). As a result, the photoproduct is photochemically consumed during irradiation of BODIPYs bearing poorer LGs (e.g., **2**, Φ_r^{deg} = 0.34%; Figures S7). Photobleaching of the photoproduct is accelerated by the absence of oxygen and the presence of heavy atoms in the molecule and might thus originate from the triplet state. In summary, these data confirm that introduction of heavy atoms at the 2,6-position of *meso*-methyl BODIPY photocages is a viable approach to increase their quantum yields of release.

***meso*-Methyl Substitution.** Next, we examined the effect of changing the primary *meso*-methyl carbon bearing a LG into a secondary carbon. This strategy has proved effective in many types of photocages, for example, in nitrobenzyl and coumarinylmethyl PPGs.[1] We hypothesized that in the case of *meso*-methyl BODIPY photocages, a secondary position would better stabilize the carbocation putatively formed during the photoreaction (Scheme 1), thus accelerating its rate and increasing its efficiency. To test this hypothesis, we synthesized derivatives **4** and **5**, which bear a methyl on the *meso*-methyl carbon (Figure 1). These BODIPY derivatives were synthesized as single enantiomers by reaction of 2,4-dimethyl-pyrrole with (*S*)-(−)-2-acetoxypropionyl chloride. In addition, we synthesized both secondary and primary BODIPYs with no substituents in the positions 1 and 7 (**7** and **8**, respectively) to evaluate the effect of possible steric interaction with the *meso*-methyl substituents. The spectroscopic properties of these six BODIPYs are summarized in Table 2 (data for **2** are repeated from Table 1 for comparison).

While the primary *meso*-methyl derivatives (**2** and **6**) exhibit strong fluorescence ($\Phi_f \approx 70\%$), the corresponding secondary BODIPY derivatives (**4** and **5**, respectively) gave a very weak fluorescence ($\Phi_f \approx 2.5\%$). This fact can be related to an out-of-plane geometry of the BODIPY core evoked by the *meso*-methyl/1,7-dimethyl groups steric hindrance, making non-radiative decay via "butterfly motion" more efficient as already reported for other substituted BODIPYs.[33] Indeed, compound **7**, in which this interaction is absent because positions 1 and 7 bear only small hydrogen atoms, exhibited a very high Φ_f value of 95.8%. To our surprise, an anticipated enhanced stability of the carbocation by methyl substitution in the *meso*-position (in **4**, **5**, and **7**) did not increase the photoreaction quantum yield (Table 2). From the data in Table 2, we can deduce that either an efficient radiation process in **7** or a nonradiative decay in **4** and **5** are the dominant pathways strongly competing with the reaction efficiency. We conclude that substitution on the *meso*-methyl carbon did not show the anticipated effects and can be avoided as a synthetically more demanding modification.

Leaving Group Quality. We found that the quality of the LG affected both the deprotection chemical yield and the reaction efficiency. This is a common observation in many PPGs,[1] and it has also been preliminarily demonstrated in the case of *meso*-methyl BODIPY photocages.[25] Because effect of the LG quality, represented by the pK_as of their conjugate acids, on the photoreaction efficiency has implications in terms of mechanistic understanding, we included it in our SAR investigation. The LGs with considerably different pK_a values, such as Cl^-, AcO^-, and MeO^- (pK_a = −7.0, 4.76, and 15.5, respectively) showed a substantial difference in the quantum efficiency of photoreaction from the corresponding molecules (Φ_r^{deg} = 2.37, 0.34, and 0.04% for **1**, **2**, and **3**, respectively). These data suggest that direct release of poor LGs, such as alcohol, amine, or thiol, would be inefficient from the *meso*-methyl BODIPY photocages and would require different chemistries for their attachment (e.g., as a carbonate for alcohols or a carbamate for amines) to facilitate effective release. As expected, a comparison of BODIPYs bearing LGs with a narrower pK_a range (2.5−4.47, Figure 1; molecules **9**−**13**) revealed much smaller and rather variable effects on the release quantum efficiency (Φ_r^{deg} = 0.41−0.77%, Table S1), even when the chemical nature of the LG was significantly different (e.g., carboxylate vs thiocarbonate). The observed variability could be attributed to a subtle interplay among electronic and structural properties of the LGs. Thus, we can conclude that the LG quality plays a dominant role in its photochemical liberation from the BODIPY photocage, which also supports our assumption of the carbocation intermediacy.

Photorelease Mechanism. Our experimental findings, especially the enhancement of Φ_r by the presence of a heavy atom, or the reduced reaction efficiency in the presence of oxygen, suggest that the triplet excited state must be at least partially responsible for release of the LG. This is also in accord with prior studies finding that halo-BODIPYs with modest LGs have improved quantum yields for photoreaction.[25,26] It was anticipated that the triplet excited state would release the LG and generate the carbocation in its triplet state[25] (Scheme 1). Therefore, $[Ru(bpy)_3]Cl_2$ was used as a triplet sensitizer, the absorption spectrum of which does not overlap with that of **1-Cl**, and its triplet energy is higher than that of **1-Cl** to allow efficient energy transfer (the bimolecular quenching constant k_q was determined to be 5.67×10^9 L mol^{-1} s^{-1}). Upon exclusive irradiation of $[Ru(bpy)_3]Cl_2$ in a mixture with **1-Cl**, an efficient LG photorelease from the BODIPY derivative was observed providing evidence that one of the productive excited states is of the triplet multiplicity (for details see Supporting Information).

We further examined the possibility that the singlet excited state is also involved in the LG release. For example, the ISC quantum yield for **1-Cl** (Φ_{ISC} = 0.12) is lower than the photoreaction quantum yield (Φ_r^{deg} = 0.2), but the reaction is quenched by the presence of oxygen ($\Phi_r^{aer} \approx 0.09$; Table 1). Provided that the triplet state is quenched completely under such circumstances, we can consider $\Phi_r^{aer} = \Phi_r^S \approx 0.09$ as an upper limit, thus $\Phi_{ISC} = \Phi_r^T = \Phi_r^{deg} - \Phi_r^{aer} \approx 0.11$. Therefore, both the singlet and triplet states of **1-Cl** give the photoproduct with similar efficiencies. The fluorescence quantum yield of **1-Cl** is relatively low (Φ_f = 0.17), especially when compared to that of the acetate **2-Cl** (Φ_f = 0.68). A similar effect was observed for fluorescence lifetimes of **1** (τ_f = 3.6 ns) and **2** (τ_f = 6.5 ns). The release of the LG (Cl^-) was found to be solely a photochemical process, no solvolysis was observed in the dark, and the quantum yield was independent of the **1-Cl** concentration and the irradiation light intensity. This excludes autocatalytic (sensitization) or photochemical chain processes. In addition, phosphorescence was not detected at room temperature. We can thus calculate the efficiency of a nonradiative decay from the S_1 state, $\Phi_{nr}^S = 1 - (\Phi_f + \Phi_{ISC} + \Phi_r^{aer}) \approx 0.62$, which is responsible for a lower reaction efficiency. This value could not be calculated accurately because we could not determine the triplet lifetime using transient spectroscopy (Φ_{ISC} is too low) as well as the efficiency of a radiationless deactivation process (Φ_{nr}^T, involving the ISC). However, because the sum of the Φ_{nr}^S, Φ_f, Φ_r^S, and Φ_{ISC} values is 0.99, Φ_{nr}^T must be very small. This is depicted in the Jabłoński

DOI: 10.1021/jacs.7b08532
J. Am. Chem. Soc. 2017, 139, 15168−15175

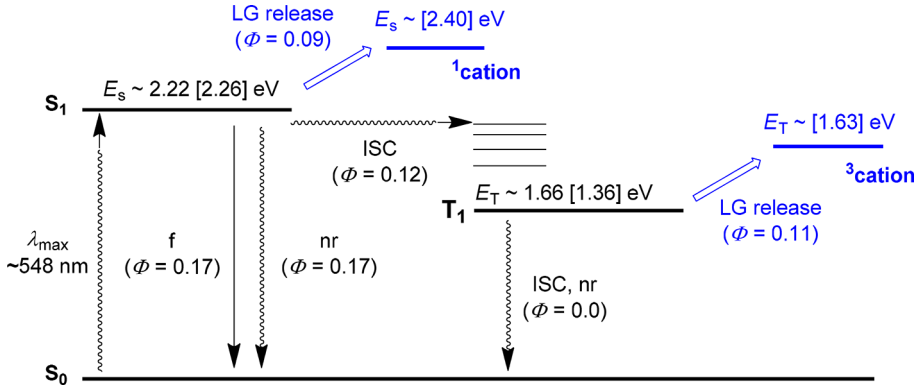

Figure 2. Jabłoński diagram of **1-Cl** photochemistry. The energy values are based on experimental spectroscopy; those in square brackets were determined theoretically. All theoretical calculations were carried out using the SMD aqueous solvation model, the S_1 energy was calculated with TD-MN15/6-31G(d), and all other theoretical values were calculated with MN15/6-31G(d). The quantum yields are taken from Table 2. f and nr stand for fluorescence and nonradiative processes, respectively.

Table 3. Photophysical Properties and Photoreaction Quantum Yields for *B*-Alkyl and *B*-Aryl BODIPYs[a]

	absorption		emission	photoreaction[b]		theoretical triplet[c]	
compd	λ_{max}^{abs}/nm	ε/M^{-1} cm^{-1}	λ_{max}^{f}/nm	Φ_r^{aer}/%	Φ_r^{deg}/%	$\Delta G^{\ddagger}$/kcal mol^{-1}	ΔG_r/kcal mol^{-1}
15	519	60 580	556	35.1 ± 4.5	68.0 ± 7.1	1.2	−2.3
16a	512	68 500	550	5.5 ± 0.2	10.8 ± 1.2	13.9	8.9
16b	513	55 300	550	4.4 ± 0.3	7.8 ± 0.8	n.d.	n.d.
16c	517	58 300	562	0.57 ± 0.02	1.1 ± 0.09	n.d.	n.d.

[a]Solutions in methanol, $c \approx (1-10) \times 10^{-6}$ M. n.d. = not determined. [b]Determined by irradiation at 507 nm using xanthene-9-carboxylic acid[23] as an actinometer. aer = aerated and deg = degassed solutions. [c]Energies are the calculated change in the Gibbs free energies using MN15/6-31G(d) and the SMD aqueous solvation model at 298 K, $\Delta G^{\ddagger}$ represents the barrier to solvolysis, and ΔG_r is the energy of the infinitely separated solvolysis products on the lowest triplet surface.

diagram in Figure 2, showing that upon excitation, the singlet excited state S_1 is formed and then deactivated by fluorescence, radiationless relaxation, and intersystem crossing to give the triplet excited state (T_1) and LG release. The energy of the S_1 state (E_S) was estimated from the 0−0 transition (Figure S8); the T_1 state energy (E_T) was estimated from the phosphorescence spectrum of a halogen-containing BODIPY.[31] The LG is released to form a *meso*-methyl cation as an intermediate possessing the multiplicity of the preceding excited state. The ion pair formed can either recombine (which may be the major nonradiative deactivation process that regenerates the starting material[25]) or be attacked by a nucleophile such as methanol to give the solvolysis product **3**. We were unable to detect the cation intermediate by transient spectroscopy as it does not accumulate in the system and might also exhibit a weak transient absorption. In summary, an excellent LG such as chloride is released from the *meso*-methyl BODIPY derivative **1-Cl** from both the singlet and triplet excited states. Its release from the T_1 state is the principal deactivation pathway, whereas the release efficiency from the S_1 state is substantially diminished by a nonradiative decay, probably ion pair recombination, and fluorescence.

As mentioned above, the photorelease quantum yields Φ_r in **1-Br** and especially in **1-I** are remarkably high (Table 2), and as a result, their Φ_{ISC} and triplet lifetimes eluded direct measurements. Therefore, we can only estimate an upper limit for $\Phi_r^T = \Phi_r^{deg} - \Phi_r^{aer}$ to be ∼0.24 and 0.36 and $\Phi_r^{aer} = \Phi_r^S$ to be 0.27 and 0.45 for **1-Br** and **1-I**, respectively, but we cannot evaluate the contribution of nonradiative processes.

In the case of BODIPYs bearing mediocre LGs (e.g., acetate in **2**; Table 2), the reaction efficiencies are relatively low. For example, if we consider $\Phi_{ISC} = 0.54$, $\Phi_r^{aer} = \Phi_r^S = 0.007$, and $\Phi_r^T = \Phi_r^{deg} - \Phi_r^{aer} = 0.008$ for **2-Br**, then Φ_{nr}^S must be relatively small (∼0.16), but Φ_{nr}^T is the major deactivation pathway from the efficiently formed T_1 state. However, the triplet lifetimes of **2-Br** in degassed, aerated, and oxygenated (purged with pure oxygen) samples were determined to be 20 μs, 250 ns, and 90 ns, respectively, which means that oxygen did not quench the triplet state fully. Thus, our original $\Phi_r^{aer} = \Phi_r^S$ premise cannot be valid, however, a too small value of Φ_r does not allow us for a more precise efficiency evaluation. We conclude that mediocre LGs open a channel for an efficient ion pair recombination and nonradiative decay from the triplet manifold.

Computations of the reaction energetics (MN15/6-31G(d), SMD = H_2O; Table 3) on the triplet excited state for **1** and **2** were performed. Although these computations are likely not quantitatively accurate due to the challenge of computing a reaction involving changes in the number of charges, they provide some qualitative insights. The ground state of the carbocations derived from **1** was computed to have both the singlet- and triplet-state energies higher than those of the corresponding excited-state levels (Figure 2). The carbocation derived from heterolysis of **1** and **2** has already been shown to have a diradical character.[25] Interestingly, the triplet state of the carbocations formed upon photorelease was computed to be the ground state, yet the isolated photoproduct is the solvent adduct. This may be analogous to what has been observed for the coumarinylmethyl photocage, where the singlet-state derived products are obtained unless the carbocation is incarcerated within a molecular container, where it is long-

DOI: 10.1021/jacs.7b08532
J. Am. Chem. Soc. 2017, 139, 15168−15175

lived enough to undergo ISC and the latent diradical behavior is observed.[34]

Overall, these mechanistic studies are consistent with a simple photoheterolysis mechanism that exhibits improved efficiencies with better LGs. Although photorelease can occur from either the singlet or triplet excited state, BODIPY compounds that favor ISC to the triplet excited state have improved quantum yields of release, either by making the excited state longer-lived or by preventing a spin-forbidden ion pair recombination.

***B*-Alkyl/Aryl BODIPY Photocages.** On the basis of the photoreaction mechanism, we hypothesized that increasing the electron density in the molecule would improve the photoreaction efficiency by stabilizing the carbocation intermediate. This hypothesis was experimentally supported by comparison of BODIPYs **1** and **14** bearing different substituents in the positions 1 and 7. The electron-donating nature of these methyl groups should increase the electron density in BODIPYs, and indeed, their absence in **14** led to a ∼1.5-fold decrease in Φ_r compared to **1** (1.04% vs 1.62%, spectroscopic data for **14** appears in Table S1). Replacement of the fluorides on the boron by alkyl chains provides an easily accessible synthetic route to further increase the electron density in BODIPYs. Indeed, computations of the reaction energetics (MN15/6-31G(d), SMD = H_2O) of boron-dimethyl BODIPY photocages **15** and **16a** (Figure 3, dimethyl analogues of compounds **1** and

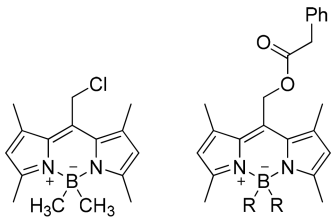

Figure 3. Structures of *B*-alkyl and *B*-aryl BODIPY derivatives.

6) showed that both *B*-dimethyl BODIPY compounds have considerably lowered transition-state barriers and more favorable reaction free energies compared to their BF_2 analogues. For **15**, bearing chloride as a LG, the release on the triplet state is computed to be downhill and nearly barrierless (Table 3 and Figure S8).

Encouraged by the calculated results, we synthesized the *B*-dimethyl BODIPY derivative bearing chloride as an excellent LG (**15**), as well as a set of three *B*-dialkyl/aryl BODIPYs bearing phenylacetic acid as a mediocre LG (**16a**–**16c**, Figure 3). In terms of photoreaction efficiency, *B*-dimethyl derivatives **15** and **16a** were up to 30-fold more reactive than their BF_2 analogues (**1** and **8**, respectively); the effect was more pronounced in the derivatives bearing a good LG (**15** vs **1**). Within the **16a**–**16c** set, a trend of inverse correlation between the *B*-substituent bulkiness and Φ_r (both in aerated and degassed solutions) was observed. This could be rationalized by a different electronic nature of the substituents and/or the fact that bulkier substituents on the boron atom are known to decrease the planarity of the BODIPY core, allowing for better nonradiative deactivation of the excited state.[33] These data confirm that alkylation of the BODIPY's boron atom is an effective approach to improving its photoreaction and that the least bulky substituent is preferred. The preference for a less bulky substituent suggests the existence of a trade-off between electron donation of the substituent, putatively increasing the Φ_r, and the extent to which it distorts the planarity of BODIPY core, which decreases Φ_r. The spectroscopic and photophysical properties of these four derivatives are presented in Table 3. The absorption spectra of the *B*-dialkyl/aryl BODIPYs are bathochromically shifted up to 14 nm compared to their BF_2 analogues, and their molar absorption coefficients are comparable. Interestingly, all *B*-dialkyl BODIPYs exhibit significant Stokes shifts (up to 1548 cm^{-1} for **16c**), unusual for BF_2–BODIPY derivatives,[35] suggesting geometrical[36] and solvation[37] changes of the excited singlet state.

Combining 2,6-Halogenation with Boron Alkylation: Substituent Effects Are Additive. Two structural motifs were identified to increase BODIPY photocage efficiency: 2,6-dihalogenation (∼7-fold increase for uncaging for **2-I** over **2**) and boron methylation (up to ∼30-fold increase for **16a** over **2**). We hypothesized that the photoreaction efficiency could be further increased by combining these two structural modifications to achieve an additive effect. Thus, we synthesized 2,6-diiodo *B*-dimethyl BODIPY photocages **17** and **18a** (Figure 4) and obtained their photophysical properties and photoreaction quantum yields (Table 4).

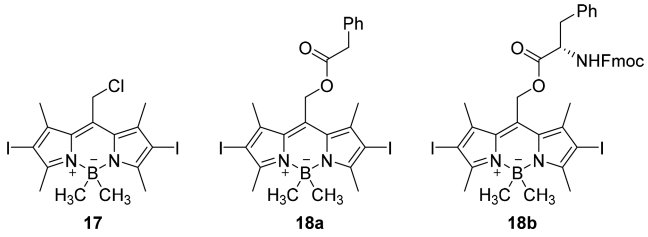

Figure 4. Structures of the *meso*-methyl BODIPY photocages featuring 2,6-diiodo and *B*-dimethyl groups.

Table 4. Photophysical Properties and Photoreaction Quantum Yields for 2,6-Diiodo *B*-Dimethyl BODIPY Photocages[a]

	absorption		emission	photoreaction[b]	
compd	λ_{max}^{abs}/nm	ε/M^{-1} cm^{-1}	λ_{max}^{f}/nm	Φ_r^{aer}/%	Φ_r^{deg}/%
17	542	62 400	573	71.9 ± 8.0	95.1 ± 10.1
18a	538	60 700	572	15.6 ± 2.1	28.1 ± 2.8
18b	537	63 000	573	32 ± 4[c]	n.d.

[a]Solutions in methanol, $c \approx (1-10) \times 10^{-6}$ M. n.d. = not determined. [b]Determined by irradiation at 507 nm using xanthene-9-carboxylic acid[23] as an actinometer. [c]Determined by irradiation at 530 nm using **18a** as an actinometer. aer = aerated and deg = degassed solutions.

Indeed, **17** and **18a** showed a significant increase in their quantum efficiencies of release compared to either their 2,6-diiodo analogues (**1-I** and **2-I**, respectively, up to 12-fold increase) or *B*-dimethyl versions (**15** and **16a**, respectively, up to ∼2.5-fold increase). The improvement in Φ_r over the original BODIPY photocages **2** was dramatic, nearly 2 orders of magnitude comparing **18a** to **2**. In addition, a caged phenylalanine derivative **18b** (Figure 4) was synthesized to demonstrate that a biologically relevant substrate can also be liberated from a BODIPY PPG. The protected phenylalanine was photoreleased with a quantum yield of 32% in an aerated methanol solution, which is even higher than that of

DOI: 10.1021/jacs.7b08532
J. Am. Chem. Soc. 2017, 139, 15168–15175

phenylacetate released from **18a** (Table 4). It is important to note that these new analogues of BODIPY photocages maintain strong absorption properties (~6×10^4 M^{-1} cm^{-1}), which, combined with their superb Φ_r, can reach Φ_r $\varepsilon(\lambda_{irr})$ of ~40 000 (!), which is ~2 orders of magnitude higher than the value reported for the best original BODIPY photocages,[25,26] and the highest value for any photocage that absorbs visible light.

CONCLUSIONS

We have evaluated the photochemical and photophysical properties of a library of BODIPY derivatives, demonstrating that high quantum yields of photorelease can be achieved with judicious selection of substituents. In particular, substituents that promote intersystem crossing and help to lower the barrier for release on the triplet excited state give exceptional quantum yields and achieve higher uncaging cross sections than other visible-light-absorbing photocages. The BODIPY scaffold is attractive for biological studies, as it features a strongly absorbing visible-light-absorbing chromophore that is simultaneously synthetically accessible, thermally stable, cell permeable, and biologically benign. Furthermore, the λ_{max} for these derivatives are all located near 532 nm, a convenient wavelength for green laser excitation with the widely available Nd:YAG laser, a wavelength that is sufficiently separated from the absorption of UV-absorbing cellular moieties to avoid phototoxicity. The best of the photocages identified here make an attractive alternative to the popular UV-absorbing *o*-nitrobenzyl photocages and their derivatives, which usually possess Φ_r $\varepsilon(\lambda_{irr})$ in the order of 100 for $\lambda_{irr} \approx 350$ nm but considerably lower values at $\lambda_{irr} > 400$ nm.[1,38] The cross sections found for the best BODIPY cages in this work (Φ_r $\varepsilon(\lambda_{irr})$ in the order of 10 000) are actually so high that they can make manipulation under ambient laboratory light difficult.

ASSOCIATED CONTENT

Supporting Information

The Supporting Information is available free of charge on the ACS Publications website at DOI: 10.1021/jacs.7b08532.

Experimental material and methods; transient absorption data; photochemical and photophysical data; reaction and barrier energies; synthetic procedures; NMR spectra; HR-MS data; steady-state absorption and fluorescence spectra; computational details, including Figures S1–S137 and Tables S1–S3 (PDF)

AUTHOR INFORMATION

Corresponding Authors

*royweinstain@post.tau.ac.il
*winter@iastate.edu
*klan@sci.muni.cz

ORCID

Arthur H. Winter: 0000-0003-2421-5578
Petr Klán: 0000-0001-6287-2742

Author Contributions

⊥P.S. and E.P. contributed equally to this work.

Notes

The authors declare no competing financial interest.

ACKNOWLEDGMENTS

Support for this work was provided by the Czech Science Foundation (GA13-25775S). The RECETOX research infrastructure was supported by the projects of the Czech Ministry of Education (LO1214 and LM2011028) (P.K.). T.S. thanks the Experientia Foundation for a postdoctoral fellowship. A.H.W. thanks the National Science Foundation (CHE-1464956), the Department of Energy (DESC0014038), and the ACS PRF (PRF55820-ND4) for support of this work. This work used the Extreme Science and Engineering Discovery Environment (XSEDE), which is supported by National Science Foundation grant number ACI-1053575, as well as the HPC@ISU equipment at Iowa State University, some of which has been purchased through funding provided by NSF under MRI grant number CBS 1229081 and CRI grant number 1205413. R.W. thanks the German-Israeli Foundation for Scientific Research and Development (I-2387-302.5/2015) and the European Research Committee (679189) for support of this work. D.K. thanks the Planning and Budgeting Committee (PBC) of the Israeli Council for Higher Education for a postdoctoral fellowship.

REFERENCES

(1) Klan, P.; Solomek, T.; Bochet, C. G.; Blanc, A.; Givens, R.; Rubina, M.; Popik, V.; Kostikov, A.; Wirz, J. *Chem. Rev.* **2013**, *113*, 119.
(2) Patchornik, A.; Amit, B.; Woodward, R. B. *J. Am. Chem. Soc.* **1970**, *92*, 6333.
(3) Sheehan, J. C.; Wilson, R. M. *J. Am. Chem. Soc.* **1964**, *86*, 5277.
(4) Givens, R. S.; Park, C.-H. *Tetrahedron Lett.* **1996**, *37*, 6259.
(5) Park, C.-H.; Givens, R. S. *J. Am. Chem. Soc.* **1997**, *119*, 2453.
(6) Givens, R. S.; Matuszewski, B. *J. Am. Chem. Soc.* **1984**, *106*, 6860.
(7) McCray, J. A.; Herbette, L.; Kihara, T.; Trentham, D. R. *Proc. Natl. Acad. Sci. U. S. A.* **1980**, *77*, 7237.
(8) Stensrud, K.; Noh, J.; Kandler, K.; Wirz, J.; Heger, D.; Givens, R. S. *J. Org. Chem.* **2009**, *74*, 5219.
(9) Amatrudo, J. M.; Olson, J. P.; Agarwal, H. K.; Ellis-Davies, G. C. R. *Eur. J. Neurosci.* **2015**, *41*, 5.
(10) Pehrson, J. R. *Proc. Natl. Acad. Sci. U. S. A.* **1989**, *86*, 9149.
(11) Solomek, T.; Wirz, J.; Klan, P. *Acc. Chem. Res.* **2015**, *48*, 3064.
(12) Zayat, L.; Noval, M. G.; Campi, J.; Calero, C. I.; Calvo, D. J.; Etchenique, R. *ChemBioChem* **2007**, *8*, 2035.
(13) Filevich, O.; Etchenique, R. *Photochem. Photobiol. Sci.* **2013**, *12*, 1565.
(14) Sebej, P.; Wintner, J.; Müller, P.; Slanina, T.; Al Anshori, J.; Antony, L. A. P.; Klan, P.; Wirz, J. *J. Org. Chem.* **2013**, *78*, 1833.
(15) Stacko, P.; Sebej, P.; Veetil, A. T.; Klan, P. *Org. Lett.* **2012**, *14*, 4918.
(16) Olson, J. P.; Banghart, M. R.; Sabatini, B. L.; Ellis-Davies, G. C. R. *J. Am. Chem. Soc.* **2013**, *135*, 15948.
(17) Fournier, L.; Gauron, C.; Xu, L.; Aujard, I.; Le Saux, T.; Gagey-Eilstein, N.; Maurin, S.; Dubruille, S.; Baudin, J.-B.; Bensimon, D.; Volovitch, M.; Vriz, S.; Jullien, L. *ACS Chem. Biol.* **2013**, *8*, 1528.
(18) Umeda, N.; Takahashi, H.; Kamiya, M.; Ueno, T.; Komatsu, T.; Terai, T.; Hanaoka, K.; Nagano, T.; Urano, Y. *ACS Chem. Biol.* **2014**, *9*, 2242.
(19) Takeda, A.; Komatsu, T.; Nomura, H.; Naka, M.; Matsuki, N.; Ikegaya, Y.; Terai, T.; Ueno, T.; Hanaoka, K.; Nagano, T.; Urano, Y. *ChemBioChem* **2016**, *17*, 1233.
(20) Nani, R. R.; Gorka, A. P.; Nagaya, T.; Kobayashi, H.; Schnermann, M. J. *Angew. Chem., Int. Ed.* **2015**, *54*, 13635.
(21) Konig, K. *J. Microsc.* **2000**, *200*, 83.
(22) Gorka, A. P.; Schnermann, M. J. *Curr. Opin. Chem. Biol.* **2016**, *33*, 117.
(23) Antony, L. A. P.; Slanina, T.; Sebej, P.; Solomek, T.; Klan, P. *Org. Lett.* **2013**, *15*, 4552.
(24) Palao, E.; Slanina, T.; Muchova, L.; Solomek, T.; Vitek, L.; Klan, P. *J. Am. Chem. Soc.* **2016**, *138*, 126.

DOI: 10.1021/jacs.7b08532
J. Am. Chem. Soc. 2017, 139, 15168–15175

(25) Goswami, P. P.; Syed, A.; Beck, C. L.; Albright, T. R.; Mahoney, K. M.; Unash, R.; Smith, E. A.; Winter, A. H. *J. Am. Chem. Soc.* **2015**, *137*, 3783.
(26) Rubinstein, N.; Liu, P.; Miller, E. W.; Weinstain, R. *Chem. Commun.* **2015**, *51*, 6369.
(27) Hatchard, C. G.; Parker, C. A. *Proc. R. Soc. London, Ser. A* **1956**, *235*, 518.
(28) Kamkaew, A.; Lim, S. H.; Lee, H. B.; Kiew, L. V.; Chung, L. Y.; Burgess, K. *Chem. Soc. Rev.* **2013**, *42*, 77.
(29) Al Anshori, J.; Slanina, T.; Palao, E.; Klan, P. *Photochem. Photobiol. Sci.* **2016**, *15*, 250.
(30) Ludvikova, L.; Fris, P.; Heger, D.; Sebej, P.; Wirz, J.; Klan, P. *Phys. Chem. Chem. Phys.* **2016**, *18*, 16266.
(31) Palao, E.; Slanina, T.; Klan, P. *Chem. Commun.* **2016**, *52*, 11951.
(32) Li, W.; Li, L.; Xiao, H.; Qi, R.; Huang, Y.; Xie, Z.; Jing, X.; Zhang, H. *RSC Adv.* **2013**, *3*, 13417.
(33) Kim, S.; Bouffard, J.; Kim, Y. *Chem. - Eur. J.* **2015**, *21*, 17459.
(34) Kamatham, N.; Da Silva, J. P.; Givens, R. S.; Ramamurthy, V. *Org. Lett.* **2017**, *19*, 3588.
(35) Loudet, A.; Burgess, K. *Chem. Rev.* **2007**, *107*, 4891.
(36) Chen, Y.; Zhao, J.; Guo, H.; Xie, L. *J. Org. Chem.* **2012**, *77*, 2192.
(37) Araneda, J. F.; Piers, W. E.; Heyne, B.; Parvez, M.; McDonald, R. *Angew. Chem., Int. Ed.* **2011**, *50*, 12214.
(38) Il'ichev, Y. V.; Schwörer, M. A.; Wirz, J. *J. Am. Chem. Soc.* **2004**, *126*, 4581.

DOI: 10.1021/jacs.7b08532
J. Am. Chem. Soc. 2017, 139, 15168−15175